Received: 20 November 2018 | Revised: 4 February 2019 | Accepted: 25 February 2019

DOI: 10.1002/pip.3132

RESEARCH ARTICLE

WILEY PROGRESS IN PHOTOVOLTAICS

High-efficiency photovoltaic modules on a chip for millimeter-scale energy harvesting

Eunseong Moon | Inhee Lee | David Blaauw | Jamie D. Phillips

Department of Electrical Engineering and Computer Science, University of Michigan, Ann Arbor, MI, USA

Correspondence
Eunseong Moon, Department of Electrical Engineering and Computer Science, University of Michigan, Ann Arbor, MI, USA.
Email: esmoon@umich.edu

Funding information
National Institutes of Health, Grant/Award Number: R01CA195655

Abstract

Photovoltaic modules at the millimeter scale are demonstrated in this work to power wirelessly interconnected millimeter-scale sensor systems operating under low-flux conditions, enabling applications in the Internet of things and biological sensors. Module efficiency is found to be limited by perimeter recombination for individual cells and shunt leakage for the series-connected module configuration. We utilize GaAs and AlGaAs junction barrier isolation between interconnected cells to dramatically reduce shunt leakage current. A photovoltaic module with eight series-connected cells and total area of 1.27 mm^2 demonstrates a power conversion efficiency of greater than 26% under low-flux near-infrared illumination (850 nm at 1 $\mu W/mm^2$). The output voltage of the module is greater than 5 V, providing a voltage up-conversion efficiency of more than 90%. We demonstrate direct photovoltaic charging of a 16-μAh pair of thin-film lithium-ion batteries under dim light conditions, enabling the perpetual operation of practical millimeter-scale wirelessly interconnected systems.

KEYWORDS

gallium arsenide, Internet of things, millimeter-scale energy harvesting, monolithic photovoltaic module, perimeter recombination, photoinduced shunt

1 | INTRODUCTION

Continued scaling of electronic systems and the proliferation of wireless sensor networks that have enabled the Internet of things (IoT)[1-3] necessitate a means of energy harvesting to achieve self-powered devices with small form factors. Photovoltaics (PV) are well known for efficient large-scale power generation and for their use in self-powered electronic devices at the macroscale. While the physical dimensions of PV devices and systems may be reduced, miniaturization to the millimeter scale presents new challenges in achieving high conversion efficiency. Furthermore, sources such as ambient indoor lighting or infrared radiation for wireless power transfer differ dramatically from solar irradiance in terms of both spectral content and flux.[4-7] Dark current and shunt conductive paths in PV cells become much more important at small dimensions and low-flux ambient indoor conditions[4-9] in comparison with typical outdoor solar irradiation (approximately a factor of 1000 lower flux than AM 1.5). High-efficiency PV cells can meet the power requirements (>50 nW/mm^2) of these systems through optimization of the spectral response in appropriate spectral windows: 425 to 650 nm for ambient indoor lighting[4] and 700 to 1100 nm for the infrared transparency window for biological tissue.[3] GaAs-based PV cells can provide outstanding performance in these desired wavelength regions because of a large shunt resistance and range of tunable bandgap energies (larger bandgap at 1.67 eV from $Al_{0.2}Ga_{0.8}As$ for indoor lighting[10] and smaller bandgap at 1.424 eV from GaAs for infrared illumination[5]) to maximize power conversion efficiency. Previously, power conversion efficiency values above 20% under white room lighting[10] at 580 lux (1.24 $\mu W/mm^2$) and above 30% under 850 nm infrared LED illumination[5] at 1 $\mu W/mm^2$ were achieved using single-junction GaAs cells.

The most critical issue in ensuring perpetual operation of systems is the overall power generation. In contrast to large-area applications,

cost per unit area is a secondary factor in millimeter-scale systems because of the small PV area (and hence, low cost). This enables the use of high-performance materials such as III-V compound semiconductors. Furthermore, to maximize energy capacity, the battery of the millimeter-scale systems often have a high open-circuit voltage, which is several times higher than the typical open circuit voltage of a single PV cell.[11] A switched capacitor network is typically used to achieve voltage up-conversion, where switching and resistive losses limit efficiency to approximately 50%.[12] Direct series/parallel connections of PV cells provide an appealing alternative for voltage up-conversion, where a PV network with over 80% power conversion efficiency has been demonstrated.[12] However, monolithic PV arrays present several challenges in minimizing losses associated to device isolation and shunt leakage paths between series connections.[9,13] Monolithic silicon PV arrays present several challenges including low voltage generation (large number of series-connected cells required to achieve desired voltage) and low optical absorption strength (thick absorber regions are required, making device isolation problematic).[9,11,14] The larger voltage generation and high optical absorption strength of GaAs and related compound semiconductors provide a much more attractive platform for monolithic PV modules. Previously, a laser power converter based on a six-cell GaAs PV module array was demonstrated at the millimeter scale with conversion efficiency greater than 52% under monochromatic illumination at 13.2 W/cm^2 (132 mW/mm^2), with efficiency limited by perimeter recombination and shunt leakage through the semi-insulating GaAs substrate.[9] In this work, we present monolithic GaAs-based PV modules at the millimeter scale operating under low-flux conditions (<10 μW/mm^2) as a means to power IoT systems or bio-implantable sensors without the requirement for DC-DC voltage up-conversion.

2 | EXPERIMENT

We used a baseline PV cell structure (Figure 1A) grown by molecular beam epitaxy (MBE) based on our previously reported high-efficiency single-junction GaAs PV cells,[5] where the critical limiting factor from exposed sidewall/perimeter recombination losses of single PV cells was dramatically reduced utilizing the ammonium sulfide chemical treatment and subsequent silicon nitride deposition. Monolithic PV arrays were constructed on semi-insulating GaAs substrates. While the semi-insulating GaAs substrate provides a high-resistivity material to facilitate series connection of PV cells, there is still a path for shunt leakage current that can degrade the fill factor, as illustrated in Figure 1B. We examined three approaches to investigate shunt current leakage:

(1) semi-insulating substrate alone, (2) p-GaAs junction barrier (500 nm thick, 10^{16} cm^{-3} doping), and (3) p-$Al_{0.3}Ga_{0.7}As$ junction barrier (400 nm thick, 5 × 10^{16} cm^{-3} doping). We simulated electrical characteristics for each approach using Synopsys Sentaurus TCAD[15] to obtain optimized parameters for layer thickness, p-type doping concentration, and Al mole fraction. We fabricated PV modules with eight single PV cells (255 μm × 595 μm) connected in series with 10-μm trenches for device isolation, as shown in Figure 2. The eight-cell series connection was designed to achieve a voltage output of approximately 5 V for direct battery charging. The PV module design also incorporated a small integrated photodiode for optical communications and the possibility to incorporate an open location to mount an external sensor (eg, pressure) for the system. We measured the electrical characteristics of the PV modules under dark and illuminated conditions using Keithley 2400 and 4200 semiconductor characterization tools. Illumination utilized a calibrated white-light LED or 850-nm near-infrared (NIR) LED. The incident LED light intensity was approximately 1 μW/mm^2 (420 lux) to simulate a reasonable indoor or subcutaneous low-flux condition that is approximately 1000 times smaller than AM 1.5 full sun conditions.[16] We studied incident light dependence by varying the irradiance in increments of 10 lux for white-light LED illumination and 100 nW/mm^2 for NIR LED illumination.

3 | RESULTS

3.1 | Junction barrier isolation

The *J-V* characteristics of fabricated PV modules with p-GaAs and p-$Al_{0.3}Ga_{0.7}As$ junction barrier isolation are shown in Figure 3 for 850-

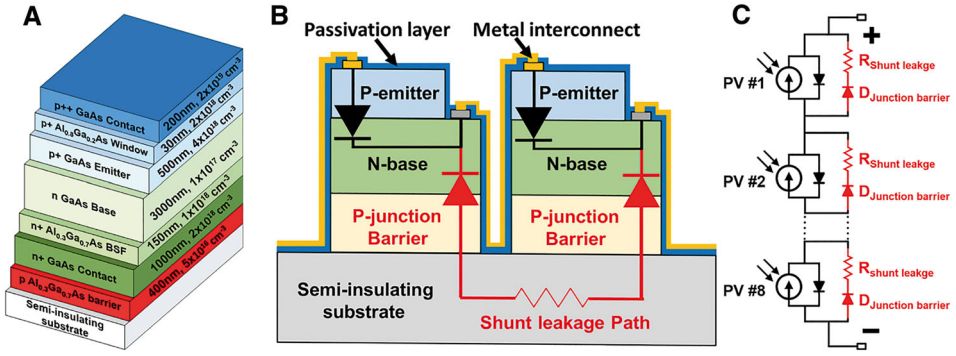

FIGURE 1 Schematic diagrams of (A) optimized epitaxial layer structure of a single cell, (B) device structure illustrating photovoltaic (PV) cell junction, junction barrier isolation, and shunt leakage path, and (C) equivalent circuit model of the PV module [Colour figure can be viewed at wileyonlinelibrary.com]

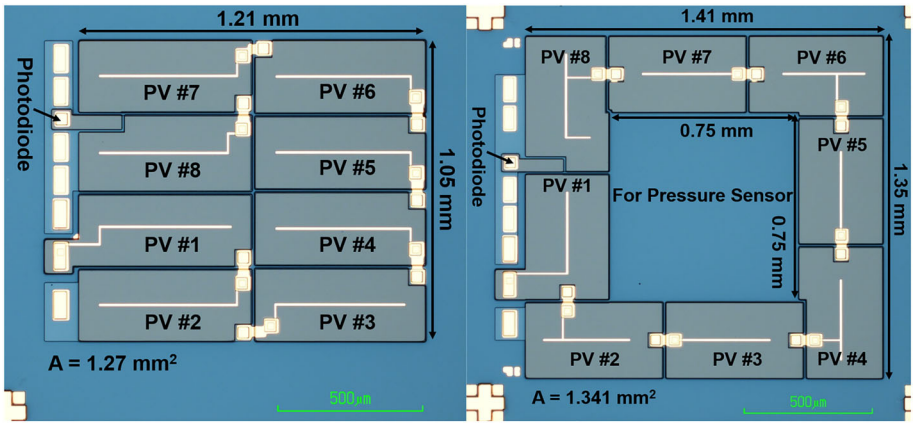

FIGURE 2 Optical microscope images of two different fabricated photovoltaic (PV) modules [Colour figure can be viewed at wileyonlinelibrary.com]

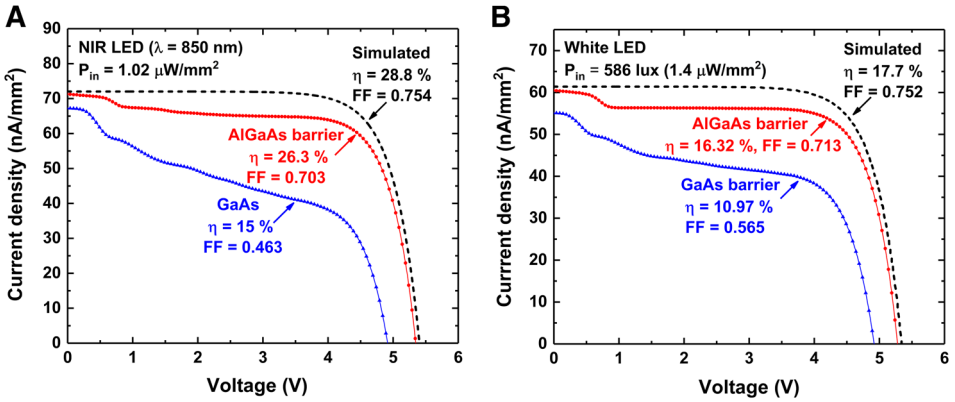

FIGURE 3 Measured *J-V* characteristics of photovoltaic (PV) modules with GaAs and AlGaAs barrier layers (A) under 850-nm near-infrared (NIR) LED illumination at 1.02 μW/mm^2 and (B) under white LED illumination at 586 lux. Comparisons are shown to simulated results (dashed) with shunt leakage removed [Colour figure can be viewed at wileyonlinelibrary.com]

nm NIR LED illumination at 1.02 μW/mm^2 and white LED illumination at 586 lux (1.4 μW/mm^2). We extracted diode parameters from single PV cells to simulate the *J-V* characteristics for series-connected cells without shunt leakage, as shown in Figure 3. PV modules with both p-GaAs and p-$Al_{0.3}Ga_{0.7}As$ junction barrier isolation produced an open circuit voltage of approximately 5 V. This voltage is near the intended design and is sufficient for direct battery charging without voltage up-conversion. The PV module with p-GaAs junction barrier isolation demonstrated a dramatic degradation in fill factor from 0.754 to 0.463 in comparison with simulated *J-V* characteristics neglecting the shunt leakage current. As a result, the overall power conversion efficiency under NIR illumination decreases from the expected value of 28.8% to 15.0% because of the inability of the GaAs junction barrier to sufficiently block shunt leakage current. We observed a dramatic improvement in performance by incorporating p-$Al_{0.3}Ga_{0.7}As$ junction barrier isolation, where the measured power conversion efficiency of 26.3% under NIR illumination compares favorably with the simulated result of 28.8% for no shunt leakage. The influence of shunt leakage on the performance of monolithic PV modules is further illustrated by the dependence of *J-V* on the number of series-connected cells (p-GaAs junction barrier isolation), as shown in Figure 4. The overall power conversion efficiency for NIR illumination demonstrates a clear decrease from 21.4% to 17.5%, with a fill factor decreasing from 0.71

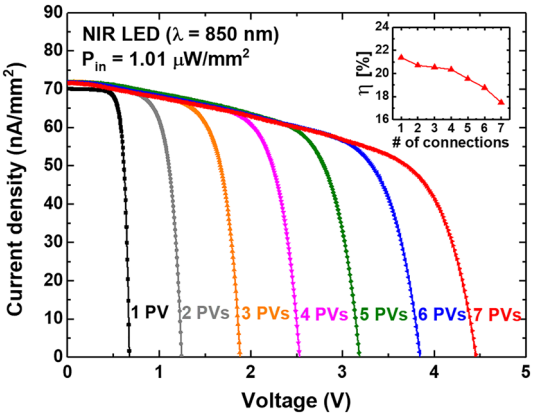

FIGURE 4 Measured *J-V* curves for varying number of photovoltaic (PV) cell series connection and (inset) corresponding power conversion efficiency at the maximum power point [Colour figure can be viewed at wileyonlinelibrary.com]

to 0.582, as the number of series connections increases from 1 to 7. The degradation in the *J-V* characteristics shows an obvious shunt leakage characteristic, as represented by the equivalent circuit model shown in Figure 1C. The *J-V* curves shown in Figure 3 are representative of our typical module characteristics, where a nonlinear current reduction is observed in the 0 to 1 V range, followed by an approximately linear shunt resistance current reduction at higher voltages. The nonlinear current reduction at lower voltage may be attributed to nonideal reverse leakage current through the junction barrier isolation. The characteristics in Figure 4 demonstrated a more conventional shunt resistance behavior without the nonlinear junction barrier leakage current at low voltage, for which the origin is unclear and is atypical for the majority of samples that we have fabricated. Further discussion of the shunt leakage behavior is described in Section 3.2.

3.2 | Characteristics of shunt leakage

We measured shunt leakage current between n-contacts of adjacent PV cells without metal interconnects under dark conditions for the three device isolation schemes, as shown in Figure 5. We observe an approximately linear *I-V* characteristic for the shunt current leakage without junction barrier isolation, suggesting that it is limited by the resistance of the semi-insulating GaAs substrate. We observe a clear reduction in shunt leakage current by incorporating p-GaAs and p-AlGaAs junction barrier isolation. The shunt leakage *I-V* characteristic for the p-GaAs junction barrier has a near exponential dependence, suggesting that leakage is mediated by the energy barrier height of the p-GaAs junction. We observe a further reduction in shunt leakage for the incorporation of a p-AlGaAs junction barrier isolation, which is near the instrument limitation of 1 pA and may be attributed to the increased energy barrier height. The energy barrier height for the three device isolation designs is illustrated in the simulated energy band diagrams shown in Figure 6. Despite the large reduction in shunt current for the addition of p-GaAs barrier isolation, there is still an

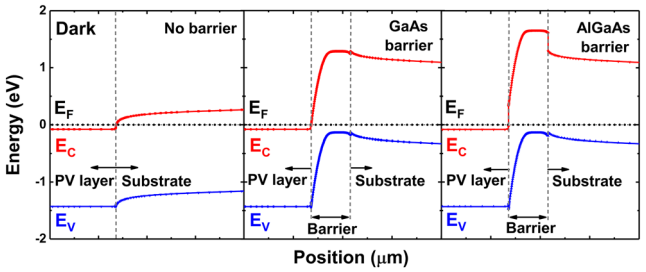

FIGURE 6 Simulated energy band diagrams between the photovoltaic (PV) cell base and semi-insulating substrate under dark conditions for three different barrier layer structures: No barrier, p-GaAs junction, and p-$Al_{0.3}Ga_{0.7}As$ junction [Colour figure can be viewed at wileyonlinelibrary.com]

obvious degradation in PV module efficiency due to shunt leakage current (Figure 3). Furthermore, for all three cases of junction barrier isolation, we observe a very low shunt leakage current that is near or below the nA range and would not be expected to dramatically impact PV module efficiency. Therefore, the shunt leakage current characteristics under dark conditions cannot fully explain our observed behavior of the PV modules under illumination.

We subsequently measured the shunt leakage current between n-contacts of adjacent single PV cells under illumination and observed a substantial increase in leakage current (Figure 7). The photo-activated behavior may be interpreted as an undesired increase in photoconductivity at the junction barrier and/or exposed regions of the semi-insulating GaAs substrate. We believe that the nonlinear bias dependence of the photo-activated leakage current may explain the nonlinear shunt leakage current observed in the modules shown in Figure 3. For all three junction isolation techniques, the shunt current increased by a factor of approximately 100. The shunt leakage for the p-GaAs junction barrier isolation rises to the level of 10 nA, comparable with the photogenerated current, resulting in the observed reduction in PV module performance due to shunt leakage. In contrast, the larger barrier height associated with our p-AlGaAs junction isolation approach significantly improves the ability to block shunt leakage

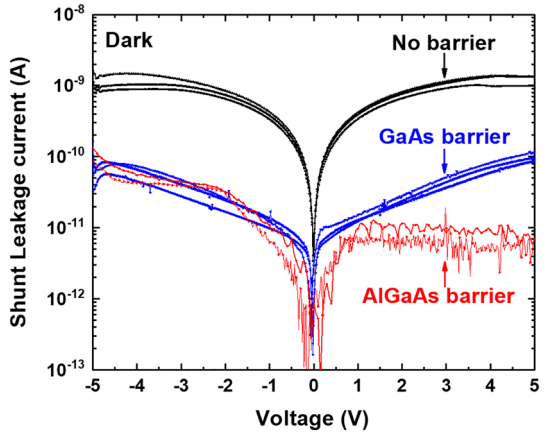

FIGURE 5 Measured shunt leakage current under dark conditions for three different barrier structures: No barrier, p-GaAs junction, and p-$Al_{0.3}Ga_{0.7}As$ junction [Colour figure can be viewed at wileyonlinelibrary.com]

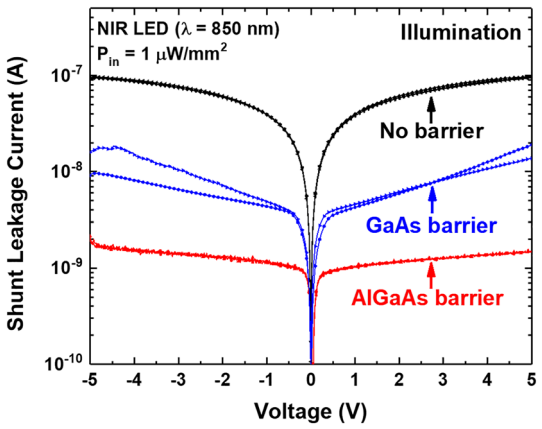

FIGURE 7 Measured shunt leakage current under near-infrared (NIR) LED illumination for three different barrier structures: No barrier, p-GaAs junction, and p-$Al_{0.3}Ga_{0.7}As$ junction [Colour figure can be viewed at wileyonlinelibrary.com]

current under illumination. The p-AlGaAs junction barrier isolation limits the shunt leakage current under illumination to approximately 1 nA, preserving the fill factor and overall power conversion efficiency of PV modules.

3.3 | Comparison of PV module performance with single PV cell

To gauge the overall power generation of the PV modules, we examined the resulting *P-V* characteristics and compared with a 6.4-mm^2 single PV cell,[5] as shown in Figure 8. The power conversion efficiency of a 1.27-mm^2 PV module with p-AlGaAs junction barrier isolation was 26.3% under 850-nm infrared LED illumination at 1.02 μW/mm^2 and 16.3% under white LED indoor conditions at 586 lux (1.4 μW/mm^2). We observed a dramatic decrease in power generation for the p-GaAs junction barrier isolation module, as expected based on the shunt leakage degradation observed in *J-V* characteristics. The power conversion efficiency of the PV module with p-AlGaAs junction barrier isolation, however, approaches the simulated result neglecting shunt leakage current. In comparison with the single PV cell, the PV module with AlGaAs junction barrier isolation provides a voltage that is approximately eight times higher, with approximately 1/8 current reduction. The voltage generated by the PV module is sufficient for direct battery charging and provides an effective voltage up-conversion efficiency of approximately 90% for both NIR and white LED illumination.

We observe a strong dependence of power conversion efficiency on incident light intensity, as shown in Figure 9 for NIR illumination. This dependence has been previously studied for small-area GaAs cells[5] and attributed to perimeter sidewall recombination. Consistent with our *J-V* and *P-V* curves, the shunt leakage current for PV modules with p-GaAs barrier junction isolation results in power conversion efficiency degradation over the full range of light intensity studied. The p-AlGaAs barrier junction isolation module demonstrates power conversion efficiency that approaches the performance of the single PV cell for the full range of illumination intensity. These results confirm that the PV module with p-AlGaAs junction barrier isolation can maintain efficiency comparable with a single PV cell under extremely dim light conditions below 100 nW/mm^2.

3.4 | Practical application of millimeter-scale PV energy harvesting

To illustrate the utility of millimeter-scale PV modules, we constructed a fully-encapsulated 17-mm^3 wireless sensor system incorporating a GaAs PV module[17] (Figure 10). The system includes a 16-μAh thin-film lithium-ion battery pair that is directly charged by the PV module

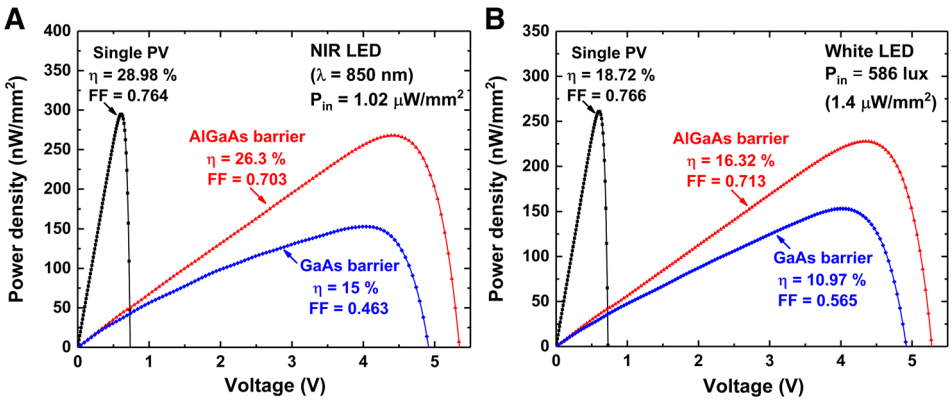

FIGURE 8 Comparison of measured *P-V* characteristics between photovoltaic (PV) arrays and single PV cell (A) under 850-nm near-infrared (NIR) illumination at 1.02 μW/mm^2 and (B) under white LED illumination at 586 lux [Colour figure can be viewed at wileyonlinelibrary.com]

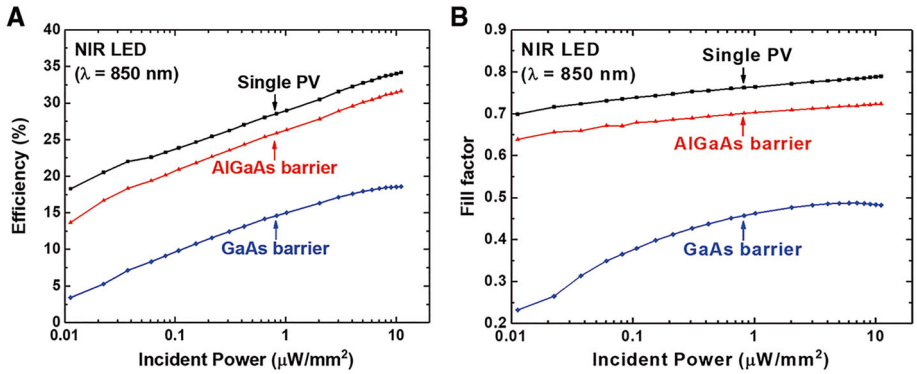

FIGURE 9 Light intensity dependence of (A) power conversion efficiency and (B) fill factor for single photovoltaic (PV) and PV modules with p-GaAs and p-AlGaAs barrier junction isolation [Colour figure can be viewed at wileyonlinelibrary.com]

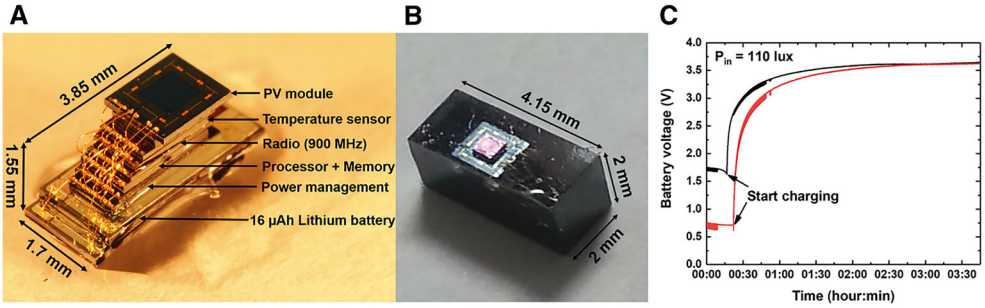

FIGURE 10 Optical microscope images of a wireless millimeter-scale sensor system with integrated PV module (A) before and (B) after encapsulation. (C) Monitored battery voltage output of this millimeter-scale system during the charging process under 110 lux indoor illumination [Colour figure can be viewed at wileyonlinelibrary.com]

through a reverse-current blocking diode. Battery charging characteristics under dim indoor illumination at 110 lux are shown in Figure 9C. The PV module demonstrates a clear recovery of battery voltage within 2 hours, providing adequate energy storage to operate the system. The average power requirement to report temperature every 30 minutes is 28.4 nW, comparing favorably with the average power generation of the PV module of 70.8 nW under 200 lux. While the PV system demonstrates the ability to power a millimeter-scale wireless sensor nodes, there are still opportunities to further improve conversion efficiency through reducing losses that appear at low light intensity[5] (eg, perimeter recombination) and losses associated with shunt leakage current for modules[9] providing voltage up-conversion.

4 | CONCLUSION

PV modules offer an efficient means for energy harvesting and direct battery charging in millimeter-scale systems. This application places unique demands on both PV cells and the module, where PV cells require high performance under much dimmer conditions than conventional solar cells, and PV modules have a critical emphasis on maximizing area and electrical isolation of adjacent cells. We demonstrated GaAs PV modules at the millimeter scale with high efficiency under low-flux conditions, where AlGaAs junction barrier isolation provided a critical step in limiting shunt leakage current between series-connected cells. We observed power conversion efficiency of 26.3% under 850-nm infrared LED illumination at 1.02 µW/mm^2 and 16.3% under white LED illumination at 586 lux (1.4 µW/mm^2), with a 90% voltage up-conversion efficiency to reach an operating voltage of 5 V for direct battery charging. We applied a monolithic PV module to demonstrate the perpetual operation of a millimeter-scale wirelessly interconnected temperature logger system. Further improvements in millimeter-scale PV module efficiency may be gained by continued improvement in reducing perimeter leakage current in small-area cells and reduction in shunt leakage through techniques such as epitaxial layer transfer to fully insulating substrates[18] or vertical multijunction designs.[19]

ORCID

Eunseong Moon https://orcid.org/0000-0003-3378-7930

REFERENCES

1. Blaauw D, Sylvester D, Dutta P, et al. IoT design space challenges: circuits and systems. In: 2014 Symposium on VLSI Technology (VLSI-Technology): Digest of Technical Papers, pp. 1–2. IEEE, 2014.
2. Nazari, Honarvar M, Mujeeb-U-Rahman M, Scherer A. An implantable continuous glucose monitoring microsystem in 0.18 µm CMOS. In: *VLSI Circuits Digest of Technical Papers, 2014 Symposium on*, pp. 1-2. IEEE, 2014.
3. Moon E, Blaauw D, Phillips JD. Subcutaneous photovoltaic infrared energy harvesting for bio-implantable devices. *IEEE Trans Electron Devices*. 2017;64(5):2432-2437.
4. Teran AS, Moon E, Lim W, et al. Energy harvesting for GaAs photovoltaics under low-flux indoor lighting conditions. *IEEE Trans Electron Devices*. 2016;63(7):2820-2825.
5. Moon E, Blaauw D, Phillips JD. Infrared energy harvesting in millimeter-scale GaAs photovoltaics. *IEEE Trans Electron Devices*. 2017;64(11):4554-4560.
6. Freunek M, Freunek M, Reindl LM. Maximum efficiencies of indoor photovoltaic devices. *IEEE J Photovoltaics*. 2013;3(1):59-64.
7. Mathews I, King PJ, Stafford F, Frizzell R. Performance of III-V solar cells as indoor light energy harvesters. *IEEE J Photovoltaics*. 2016;6(1):230-235.
8. Araujo GL, Marti A. Limiting efficiencies of GaAs solar cells. *IEEE Trans Electron Devices*. 1990;37(5):1402-1405.
9. Kimovec R, Helmers H, Bett AW, Topič M. Comprehensive electrical loss analysis of monolithic interconnected multi-segment laser power converters. *Prog Photovolt Res Appl*. 2019;27:199–209.
10. Teran AS, Wong J, Lim W, et al. AlGaAs photovoltaics for indoor energy harvesting in mm-scale wireless sensor nodes. *IEEE Trans Electron Devices*. 2015;62(7):2170-2175.
11. Moon E, Blaauw D, Phillips JD. Small-area Si photovoltaics for low-flux infrared energy harvesting. *IEEE Trans Electron Devices*. 2017;64(1):15-20.
12. Lee I, Lim W, Teran A, Phillips J, Sylvester D, Blaauw D. A >78%-efficient light harvester over 100-to-100klux with reconfigurable PV-cell network and MPPT circuit. In: *Digest of technical papers/IEEE International Solid-State Circuits Conference. IEEE International Solid-State Circuits Conference*, vol. 2016, p. 370. NIH Public Access, 2016.

13. Pena R, Algora C. The influence of monolithic series connection on the efficiency of GaAs photovoltaic converters for monochromatic illumination. *IEEE Trans Electron Devices*. 2001;48(2):196-203.

14. Takeshiro Y, Okamoto Y, Mita Y. Mask-programmable on-chip photovoltaic cell array. *J Phys: Conf Ser*. 2018;1052(1):012144. IOP Publishing.

15. Synopsys. *Sentaurus TCAD Version K-2015.06*. Mountain View, CA: Synopsys Inc; 2015.

16. Riordan C, Hulstron R. What is an air mass 1.5 spectrum? (Solar cell performance calculations). In: *Photovoltaic Specialists Conference, 1990., Conference Record of the Twenty First IEEE*, pp. 1085–1088. IEEE, 1990.

17. Lee I, Kim G, Moon E, et al. A 179-lux energy-autonomous fully-encapsulated 17-mm 3 sensor node with initial charge delay circuit for battery protection. In: 2018 IEEE Symposium on VLSI Circuits, pp. 251–252. IEEE, 2018.

18. Gai B, Sun Y, Lim H, et al. Multilayer-grown ultrathin nanostructured GaAs solar cells as a cost-competitive materials platform for III-V photovoltaics. *ACS Nano*. 2017;11(1):992-999.

19. Datas A, Linares PG. Monolithic interconnected modules (MIM) for high irradiance photovoltaic energy conversion: a comprehensive review. *Renew Sustain Energy Rev*. 2017;73:477-495.

How to cite this article: Moon E, Lee I, Blaauw D, Phillips JD. High-efficiency photovoltaic modules on a chip for millimeter-scale energy harvesting. *Prog Photovolt Res Appl*. 2019;27:540–546. https://doi.org/10.1002/pip.3132